5th International Symposium on Three-Dimensional Electromagnetics
Sapporo, Japan, May 7–9, 2013

A 3D magnetotelluric study of the basement structure in the Mygdonian Basin (Northern Greece) including galvanic distortion correction.

Anna Avdeeva[1,2], Maxim Yu. Smirnov[3], Alexandros S. Savvaidis[4], Marcus Gurk[5] and Laust B. Pedersen[6]
[1] GEOMAR, Germany
[2] now at: University of Leicester, UK
[3] University of Oulu, Finland
[4] Institute of Engineering Seismology and Earthquake Engineering (ITSAK), Greece
[5] Institute of Geophysics and Meteorology, University of Cologne, Germany
[6] University of Uppsala, Sweden

SUMMARY

During 2006 and 2007 a total number of 90 magnetotelluric sites were deployed in the Mygdonian basin (Northern Greece) to examine the basement structure and to give new information about the top-of-basement depth for wave propagation models. Here we use both 2D and 3D inversion to analyze the data and compare the results. Overall, the structure of the basement is fairly well revealed by the data and our 3D inversion with distortion correction demonstrates that galvanic distortion is not a major issue for these data. Furthermore, the models obtained from these inversions agree well and clearly show the depth to the top of the basement. The top-of-basement depths also agree with information from boreholes available in the area, which gives additional confidence in our interpretation.

Keywords: magnetotellurics, inversion, top-of-basement

INTRODUCTION

The Mygdonian basin, situated between the two lakes Volvi and Lagada ca. 45 km north-east of Thessaloniki (Figure 1), is a neotectonic graben structure (5 km wide) with increased seismic activity along distinct normal fault patterns (Goldsworthy et al., 2002; Karagianni et al., 1999). Fluvioterrestrial and lacustrien sediments (approximately 200-600 m thick) overlie the basement consisting of gneiss-schists.

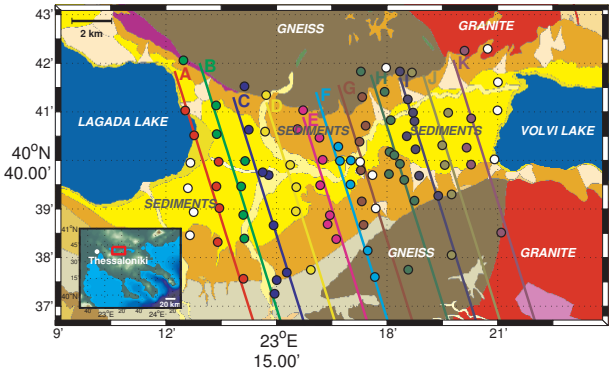

Figure 1. Geological map of the study area with MT site locations (circles), 2-D profiles (A - K) and geological outlines. For 2D inversion the sites were projected onto the profiles of the same color. The data from sites marked in white were not used for 2D and 3D inversions.

During the project "Euroseistest Volvi-Thessaloniki", a European Test site for Engineering Seismology was deployed in order to study velocity cross sections across the funnel shaped valley. In this context, the electromagnetic (EM) survey intends to map the top-of-basement to support the seismic wave propagation modeling process and site effect assessment (Manakou et al., 2010; Raptakis et al., 2005).

DATA

During 2006/2007 a total number of 90 magnetotelluric (MT) sites were installed on a roughly regular grid (North-South and East-West) in the Mygdonian basin (Figure 1), reflecting the predominant East-West orientation of many normal faults in this area. The site spacing on this grid is about 1 km. However, some areas in the mountains and around villages are not covered due to increased EM noise or due to their inaccessibility. MT data were collected using three Uppsala type MTU2000 instruments (Smirnov et al., 2008) combined with Metronix MFS05 coils. One of the instruments was used to provide a remote reference site during the entire survey. Due to the limited amount of induction coils available, we were not able to collect the vertical magnetic field at each site.

Based on this survey design we have obtained reliable estimates of the MT transfer function in the period range from $T = 0.001$ s to 1 s for day time recordings and from $T =$

0.001 s to 1000 s for the sites where both day and night recordings were available. The time series have been processed with the robust remote reference code by Smirnov (2003). All permutations of remote reference sites from inside and outside of the study area were used to estimate transfer functions. Also several time segments for 1 kHz and 3 kHz recordings were processed independently and thereafter averaged together with long period data to obtain the final transfer functions estimates. During robust averaging using the reduced M-estimator we calculated new error bars based on the bootstrap method.

Generally the data are of good quality. However, before the inversion MT transfer functions were carefully examined. The main impedance components as well as Berdichevsky's determinant averages were tested for consistency using 1D inversion. After this procedure MT data from 77 sites in a period range from $T = 0.004$ s to 5.6 s were selected for 2D and 3D inversions.

3D INVERSION

We use the 3D MT integral equation (IE) code *x*3D*i* (see Avdeeva et al. (2012)). This code resolves not only the 3D conductivity distribution in the subsurface, but also the frequency-independent elements of the full galvanic distortion matrix at each site. For the inversion the study volume is discretized by $75 \times 75 \times 22$ cells covering an area of $25 \times 25 \times 7$ km^3. All cells in horizontal directions have an area of $dx \times dy = 333 \times 333$ m^2, the vertical cell sizes are growing with depth from $dz_1 = 25$ m to $dz_{15} = 2$ km. We use 8 periods in the range from 0.004 to 5.6 s and assume a 100 Ωm half-space as an initial model.

In the code the data misfit has the following form:

$$\varphi_d = \frac{1}{2} \sum_{i=1}^{N_S} \sum_{j=1}^{N_T} \beta_{ij} \operatorname{tr} \left[\overline{(\mathbf{C}_i \mathbf{Z}_{ij} - \mathbf{D}_{ij})}^T (\mathbf{C}_i \mathbf{Z}_{ij} - \mathbf{D}_{ij}) \right] \tag{1}$$

Here, superscript T means transpose, the overbar stands for the complex conjugate and $\operatorname{tr}[\cdot]$ is the trace of its matrix argument; $\mathbf{Z}_{ij}$ and $\mathbf{D}_{ij}$ denote the 2×2 complex-valued matrices of predicted and observed impedances, respectively, $\mathbf{C}_i$ are 2×2 real-valued distortion matrices, and N_S is the number of observation sites, N_T is the number of frequencies, and β_{ij} are positive weights. In addition to distortion correction, another difference of this inversion code compared to most other codes is that for each site and frequency there is only one weight

$$\beta_{ij} = \frac{1}{N_S N_T} \left\{ \operatorname{tr} \left[\overline{(\boldsymbol{\delta}\mathbf{D})}_{ij}^T (\boldsymbol{\delta}\mathbf{D})_{ij} \right] \right\}^{-1}, \tag{2}$$

where $\delta D_{xx} = \max(\sigma(|D_{xx}|), m\,|D_{xx}|)$. The scalar m is the error floor in percent and $\sigma(|D_{xx}|) = \sqrt{\mathrm{Var}(|D_{xx}|)}$ is the standard deviation of $|D_{xx}|$. δD_{xy}, δD_{yx} and δD_{yy} are computed in a similar way.

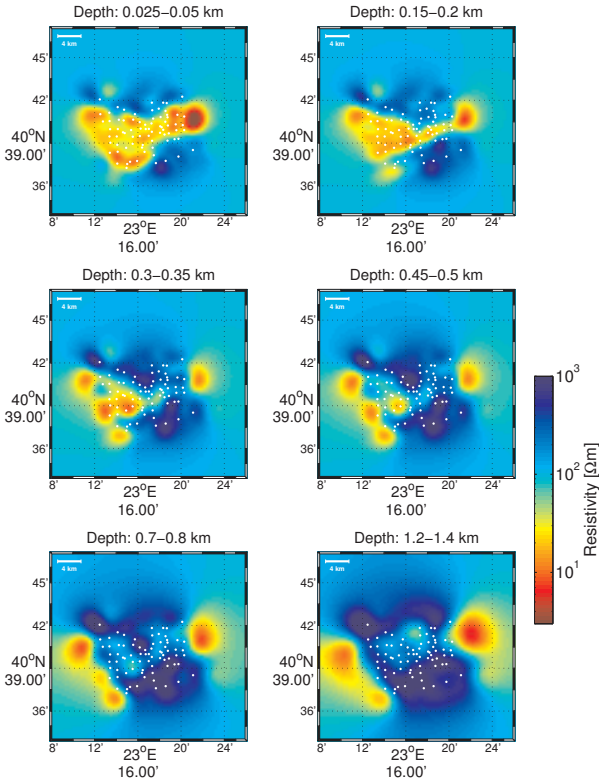

Figure 2. 3D inversion result. We correct for galvanic distortion within the inversion process. The panels show horizontal slices through the model. The depths of the slices are written above each panel.

We performed many inversion runs with various values for the error floor (1%, 5% and 10%). When the error floor is 1% the result is erratic with many artifacts and it is impossible to fit the data to a desired level. The inversion results with 5% and 10% error floor look very similar, with final RMS values of ≈ 1.5 and 1, respectively. In the following we only show the results of the inversion with 5% error floor. Figure 2 presents horizontal slices through the inversion result. The resistivity of the lacustrian sediments (≈ 20 Ωm) in the valley contrasts with the higher resistivities of the basement rocks allowing to map the structures at near surface ($z = 25 - 50$ m) in very good agreement to the geological setting as displayed in Figure 1. In a larger depth range at $z = 150 - 200$ m, the sediments at the Eastern side of the study area start to vanish. Starting from a depth of $z = 300$ m the sediments in the Eastern part of the area are not seen anymore, while in the Western part sediments are still visible. At a depth of $z = 450$ m only sediments in the South Western part of the valley are still recognizable, the basement uplift or swell in the middle of the valley is now fully developed and the sediments can be considered as almost gone.

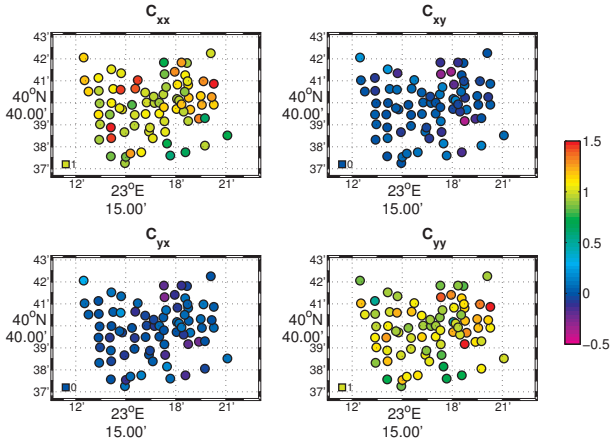

Figure 3. The elements of the resolved distortion matrix, shown as circles at the location of the MT sites. The color of each circle corresponds to the value of the element of the matrix. The square markers at the South-western side of the maps are for color reference.

The resolved elements of the Distortion matrices $\mathbf{C}_i$ are shown in Figure 3. Overall, the distortion is not very large. The matrices are very close to identity matrix for most of the stations, however there are a few stations where the data are distorted. The locations of these stations are random and there is no correlation with topography of the area.

VERIFICATION OF 3D INVERSION RESULT

We also ran 2D inversions of the data from the same 77 MT sites and within the same period range. These were performed along 11 parallel profiles (A-K), shown in Figure 1. Each MT site was projected onto the profile with corresponding color. In order to perform 2D inversion we follow the strategy by Pedersen and Engels (2005) to invert the determinant of the impedance tensor. The inversion of the determinant data has several advantages. First of all, galvanic distortions just shift the apparent resistivity values and leave the phase data unchanged, hence the determinant phase is free of galvanic distortions. Also any variability in strike direction with period does not affect the results as much as for bi-modal inversion, when proper mode decomposition is vital. Finally, determinant data does not require rotation into strike direction as it is an invariant. For the 2D inversion we adopted error floors equal to 5% for the impedance phase and 50% for the apparent resistivities. Since there was no other information in order to constrain the static shift effect and the site spacing is relatively small, we have chosen a higher error floor for the resistivity data compared to the phases to allow the inversion procedure to have more freedom to compensate for these effects. Finally, a homogeneous halfspace of 100 Ωm was used for the initial and a-priori model for the 2D inversions. This procedure resulted in an overall good fit of the observed data (RMS = 1).

The comparison of 2D and 3D inversion results for all the profiles A - K is presented in the Figure 4. The differences between 2D and 3D inversion results are very minor. The top-of-basement can be well recognized for both of these inversion results (the transition from yellow to blue).

THE TOP-OF-BASEMENT

Due to the changing hydrogeological conditions, which leads to different ranks of weathering of the basement rocks, we cannot allocate a unique resistivity value to the top-of-basement. Nevertheless, we can use available information from boreholes (Veranis, 2010) to define the resistivity range and the depth to the basement rocks at specific locations. We currently have data from 43 boreholes over the study area. Unfortunately, only 16 of them reached the basement rock. Taking the available information into account, we chose a resistivity of 60 Ωm to correspond to the top-of-basement. Figure 5 shows the distribution of the depths to the top-of-basement derived from our 3D inversion result. The agreement between the borehole data and our model is good. There are three areas, marked with letters A, B and C, where our model does not agree with the information from the boreholes. Around area C we should not trust our model since this area is not covered with MT sites. The borehole at B indicates that the top-of-basement is below 200 m, however our model suggests a shallower depth. Area A has two boreholes, that reach the basement. The deep borehole reached basement at 407 m, while our model indicates that the basement rock is at around 500 m. This could be explained by regularization, which pulls down the conductive structure. The shallower borehole shows a very sudden change in the depth to the basement rock, which is difficult to achieve with a smooth inversion strategy. The boreholes that did not reach the basement indicate that the top-of-basement is somewhere below the maximum borehole depth. These boreholes also support our interpretation.

CONCLUSIONS

We performed 2D and 3D inversion of the magnetotelluric data available in the Mygdonian basin (Northern Greece) to gain knowledge about the basement structure. Both inversion results are very similar and clearly show the depth to the basement rock. The elements of the distortion matrix retrieved by our 3D inversion algorithm show that the data are not much affected by galvanic distortion. Our interpretation also agrees well with the information available from boreholes.

ACKNOWLEDGMENTS

The authors thank Oliver Ritter for his support to this work.

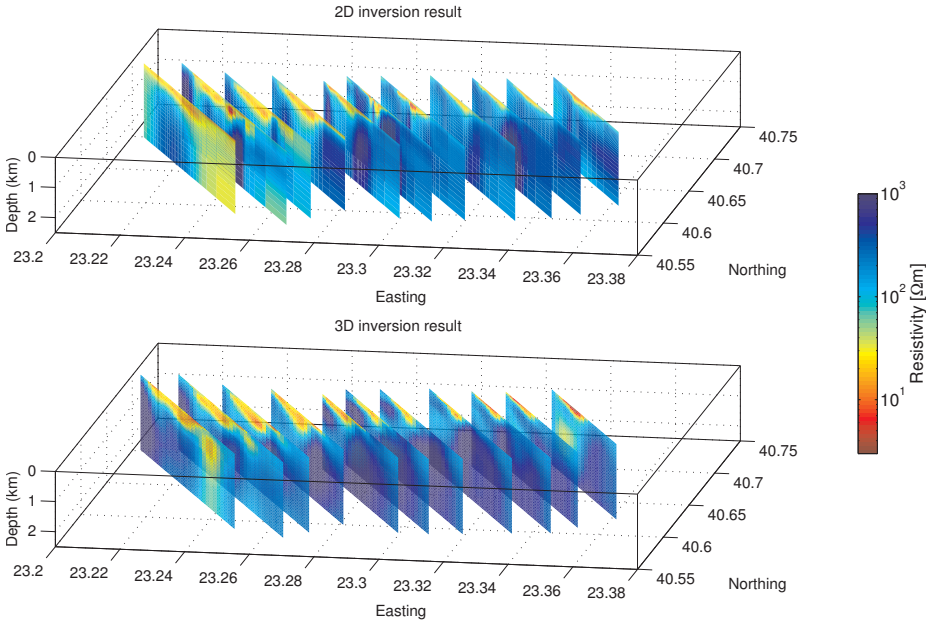

Figure 4. Comparison of the 2D and 3D inversion results.

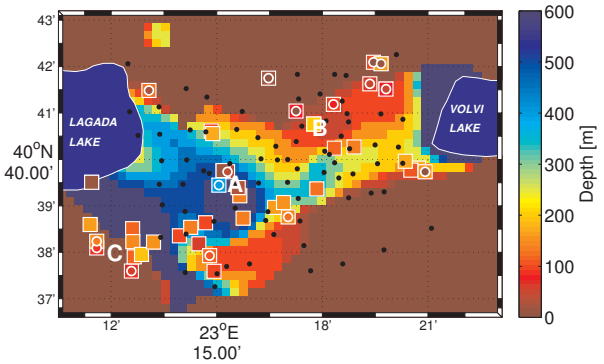

Figure 5. Comparison of top-of-basement derived from MT data with the information from the boreholes. The colored circles show top-of-basement from the boreholes which reach the basement. Squares present the maximum depth of the boreholes. Black dots are the MT sites.

REFERENCES

Avdeeva, A. D., Moorkamp, M., Avdeev, D. B., & Jegen, M. (2012). Three-dimensional inversion of magnetotelluric impedance tensor data and full distortion matrix. *Geophysical Journal International*, *under review*.

Goldsworthy, M., Jackson, J., & Haines, J. (2002). The continuity of active fault systems in Greece. *Geophysical Journal International*, *148*, 596–618.

Karagianni, E. E., Panagiotopoulos, D. G., Papazachos, C. B., & Burton, P. W. (1999). A study of shallow crustal structure in the Mygdonia Basin (N. Greece) based on the dispersion curves of Rayleigh waves. *Journal of the Balkan Geophysical Society*, *2*, 3–14.

Manakou, M. V., Raptakis, D. G., Chaŕez-García, F., Apostolidis, P., Pitilakis, & K.D. (2010). 3D soil structure of the Mygdonian basin for site response analysis. *Soil Dynamics and Earthquake Engineering*, *30*, 1198–1211.

Pedersen, L. B., & Engels, M. (2005). Routine 2D inversion of magnetotelluric data using the determinant of the impedance tensor. *Geophysics*, *70*, G33–G41.

Raptakis, D., Manakou, M., Chávez-García, F., Makra, K., & Pitilakis, K. (2005). 3D configuration of Mygdonian basin and preliminary estimate of its site response. *Soil dynamics and Earthquake Engineering*, *25*, 871–887.

Smirnov, M. (2003). Magnetotelluric data processing with a robust statistical procedure having a high breakdown point. *Geophysical Journal International*, *152*, 1–7.

Smirnov, M., Korja, T., Dynesius, L., Pedersen, L. B., & Laukkanen, E. (2008). Broadband magnetotelluric instruments for near-surface and lithospheric studies of electrical conductivity: A Fennoscandian pool of magnetotelluric instruments. *Geophysica*, *44*(1–2), 31–44.

Veranis, N. (2010). *Hydrogeological study of the grannular aquifer system of Mygdonia.* (Un. report IGME, Thessaloniki, 146 pp, maps, sections)